DALTON

Reactions of $(F_3CP)_4$ and $(F_3CP)_5$ with ruthenium and osmium carbonyl clusters: characterisation and crystal structures of the products

How-Ghee Ang,*[,a] Kiam-Wee Ang,[a] Siau-Gek Ang[a] and Arnold L. Rheingold[b]

[a] *Department of Chemistry, National University of Singapore, Lower Kent Ridge, Singapore 0511, Republic of Singapore*

[b] *Department of Chemistry and Centre for Catalytic Science and Technology, University of Delaware, Newark, Delaware 19716, USA*

The reactions of tetrameric $(F_3CP)_4$ and pentameric $(F_3CP)_5$ with $[Os_3(CO)_{11}(MeCN)]$ gave $[(OC)_{11}Os_3(\mu\text{-}PHCF_3)Os_3(CO)_{11}(\mu\text{-}H)]$ **1** while the reaction with $[Os_3(\mu\text{-}H)_2(CO)_{10}]$ led to the formation of $[Os_3(\mu\text{-}H)(\mu\text{-}PHCF_3)(CO)_{10}]$ **2** and $[(OC)_9(\mu\text{-}H)_2Os_3(\mu_4\text{-}F_3CPPCF_3)Os_3(\mu\text{-}H)_2(CO)_9]$ **3**. Pyrolysis of $(F_3CP)_4$ with $[Os_3(CO)_{12}]$ at 209 °C resulted in cleavage of the triosmium parent cluster to afford $[Os_4(CO)_{13}(\mu_3\text{-}PCF_3)_2]$ **4**. When the cyclophosphanes reacted with $[Ru_3(CO)_{12}]$ in 1 : 1 and 1 : 2 molar ratio, $[\{Ru(CO)_3(\mu_3\text{-}PCF_3)\}_4]$ **5** and $[Ru_5(CO)_{15}(\mu_4\text{-}PCF_3)]$ **6** were obtained respectively. The complex $[Ru_4(CO)_{14}(\mu_4\text{-}PCF_3)]$ **7** was obtained when the reaction between $[Ru_3(CO)_{12}]$ and $(F_3CP)_n$ (n = 4 or 5) was carried out at 80 °C. However, when $[Ru_4H(CO)_{12}]$ was treated with the cyclophosphanes the novel molecule $[Ru_4(\mu\text{-}H)_2(CO)_{12}(\mu\text{-}PCF_3)(\mu_3\text{-}PCF_3)_2]$ **8** was obtained. The crystal structures of **3**–**8** have been determined.

Early studies on the chemistry of cyclophosphanes were centred on the co-ordination characteristics with mononuclear transition-metal carbonyls.[1,2] Reaction between $(RP)_4$ (R = Ph or Et) and $(RP)_5$ (R = Ph or Me) with $[M(CO)_6]$ (M = Cr, Mo or W) resulted in substitution products such as the monodentate ligand complex $[M(CO)_5\{(PR)_5\}]$, bidentate ligand complex $[M(CO)_4\{(PR)_5\}]$ or tridentate ligand complex $[M(CO)_3\{(PR)_5\}]$. However, $P_4Bu^t_4$, a cyclophosphane containing bulky substituents, underwent ring rupture with $[Ru_3(CO)_{12}]$ and $[Ru_4H_4(CO)_{12}]$[3] to give $[Ru_5(CO)_{15}(PBu^t)]$ and $[Ru_6H_2(CO)_{12}(PBu^t)_3]$ respectively. It was also found that the reactions of $P_4Bu^t_4$ with $[Ru_3(CO)_{12}]$ using a 3 : 1 molar ratio afforded several other cluster derivatives: $[Ru_9H_3(CO)_{20}P(PBu^t)_3]$, $[Ru_7(CO)_{14}(PBu^t)_4]$, $[Ru_6(CO)_{11}(PBu^t)_4]$, $[Ru_3(CO)_7(PBu^t)_4]$ and $[Ru_4(CO)_8(PBu^t)_4]$.[4] We recently found that the reactions of pentameric cyclophenylphosphane with osmium clusters afforded a series of compounds in which the cyclophosphane ring remained intact. With $[Os_3(CO)_{11}(NCMe)]$, $(PhP)_5$ gave $[Os_3(CO)_{11}\{(PPh)_5\}]$ and $[\{Os_3(CO)_{11}\}_2\{(PPh)_5\}]$, while with $[Os_3(CO)_{10}(NCMe)_2]$ it gave $[Os_3(CO)_{10}\{(PPh)_5\}]$.[5] With ruthenium carbonyl clusters $[Ru_3(CO)_{12}]$ and $[Ru_3(CO)_{10}(NCMe)_2]$, $[Ru_4(CO)_{10}(\mu_3\text{-}PPh)_2\{\mu_4\text{-}(PPh)_2\}]$, $[Ru_4(CO)_8(\mu\text{-}PHPh)_2(\mu_4\text{-}PPh)\{\mu_4\text{-}(PPh)_2\}]$ and $[Ru_3(CO)_{10}\{(PPh)_5\}]$[6] were obtained. We now report a study involving the reactions of $(F_3CP)_4$ and $(F_3CP)_5$ with several metal clusters, $[Os_3(CO)_{11}(MeCN)]$, $[Os_3(\mu\text{-}H)_2(CO)_{10}]$, $[Os_3(CO)_{12}]$, $[Ru_3(CO)_{12}]$ and $[Ru_4(\mu\text{-}H)_4(CO)_{12}]$, in order to compare the reactivities of cyclophosphanes containing electronegative CF_3 substituents.

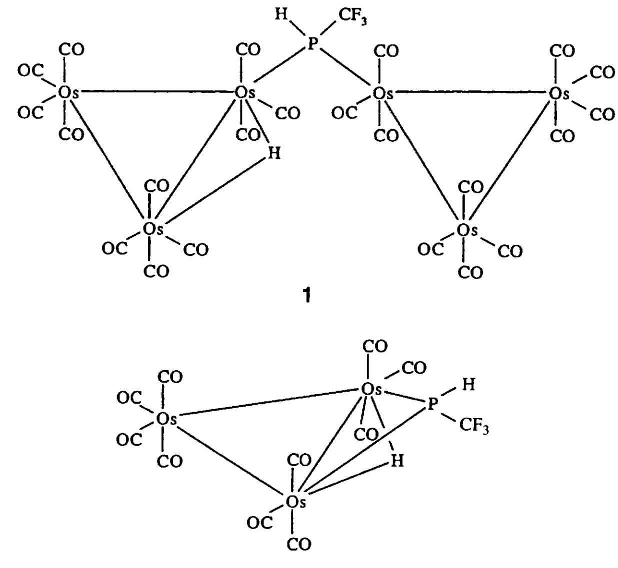

1

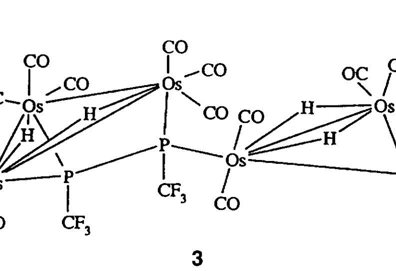

2

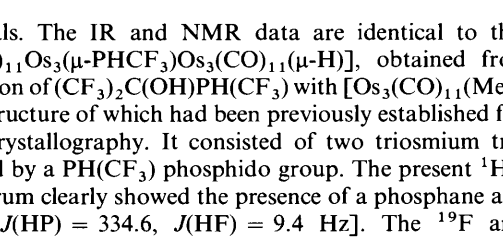

3

Results and Discussion

The reactions of the various metal carbonyl clusters with $(F_3CP)_n$ (n = 4 or 5) were carried out *in vacuo*. The products display a wide range of structural types with the ligand acting as an F_3CP moiety in μ, μ_3 and μ_4 bonding mode and as a diphosphinidene.

Reaction with $[Os_3(CO)_{11}(MeCN)]$

Treatment of $[Os_3(CO)_{11}(MeCN)]$ with an equimolar amount of $(F_3CP)_4$ in CH_2Cl_2 at 80 °C yielded complex **1** as orange crystals. The IR and NMR data are identical to those of $[(OC)_{11}Os_3(\mu\text{-}PHCF_3)Os_3(CO)_{11}(\mu\text{-}H)]$, obtained from the reaction of $(CF_3)_2C(OH)PH(CF_3)$ with $[Os_3(CO)_{11}(MeCN)]$,[7] the structure of which had been previously established from X-ray crystallography. It consisted of two triosmium triangles linked by a $PH(CF_3)$ phosphido group. The present ^1H NMR spectrum clearly showed the presence of a phosphane at δ 5.95 [dq, J(HP) = 334.6, J(HF) = 9.4 Hz]. The ^{19}F and ^{31}P

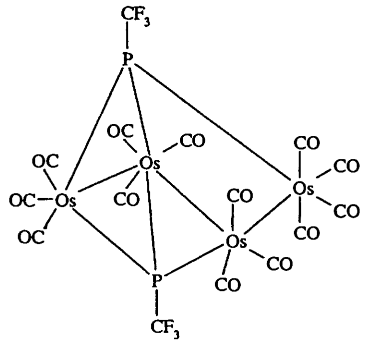

4

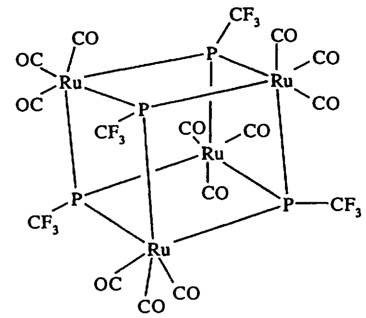

5

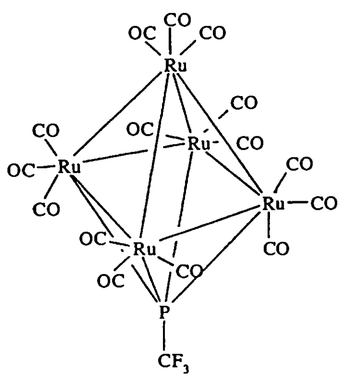

6

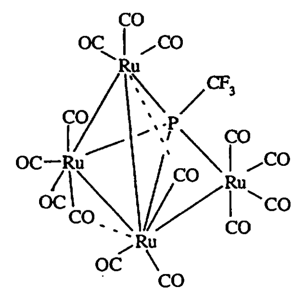

7

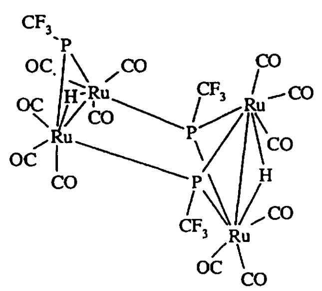

8

NMR peaks were located at δ 25.45 [dd, J(FP) = 43.9, J(HF) = 9.7] and −132.93 [q, J(FP) = 43.9 Hz] respectively, reaffirming the presence of the trifluoromethyl phosphane.

Reaction with [$Os_3(\mu\text{-}H)_2(CO)_{10}$]

Reaction of $(F_3CP)_4$ with [$Os_3(\mu\text{-}H)_2(CO)_{10}$] in hexane at 80 °C afforded complex **2**, a phosphido-bridged cluster [7] and a novel red hexaosmium compound **3**. Complex **2** showed IR and NMR data identical to [$Os_3(\mu\text{-}H)(\mu\text{-}PHCF_3)(CO)_{10}$] which was also previously obtained from the reaction of $(CF_3)_2$-C(OH)PH(CF_3) with [$Os_3(CO)_{11}(MeCN)$].[7] It is a tri-osmium cluster with the trifluoromethylphosphane and a metal hydride bridging the same Os–Os edge. The ^{1}H NMR spectrum of **3** showed signals at δ −10.19 [d, J(HP) = 6.8], −10.74 [dd, J(HP) = 7.1 Hz] and −19.32 (br, s), while the ^{19}F NMR signals are at δ 18.44 [d, J(FP) = 63.5] and 21.66 [d, J(FP) = 48.8 Hz]. The ^{31}P-{^{1}H} NMR spectrum contained two doublets of quartets at δ −57.75 [dq, J(PP) = 240.8, J(FP) = 63.5] and −81.02 [dq, J(PP) = 240.6, J(FP) = 48.7 Hz]. The ^{1}H NMR data confirmed that there were metal hydrides present in the molecule; their location will be discussed in the section on the molecular structure. The ^{31}P-{^{1}H} NMR data clearly indicated two distinct types of P while the large coupling constant of 240 Hz pointed to a P–P bond. The set of signals at δ 57.75 is assigned to P(2), that at δ −81.02 to P(1) (see Fig. 1). This assignment is supported by the fact that the bridging P in **2** has a larger coupling constant of 68.4 Hz, whereas in **1**, a P linking two triosmium triangles has a smaller coupling constant of 43.9 Hz.

Reaction with [$Os_3(CO)_{12}$]

Pyrolysis of $(F_3CP)_4$ with [$Os_3(CO)_{12}$] at 209 °C for 16 h afforded complex **4** upon TLC of the reaction mixture. The ^{19}F NMR spectrum showed signals at δ 28.19 [d, J(FP) = 61.0] and 21.67 [d, J(FP) = 51.3 Hz] while the ^{31}P NMR signals were at δ 167.90 [dq, J(PP) = 60.2, J(FP) = 59.2] and −150.74 [dq, J(PP) = 51.5, J(FP) = 49.7 Hz]. The magnitude of the ^2J(PP) and J(FP) couplings were comparable, resulting in overlapping of the two sets of signals. No ^{1}H NMR signals were observed, indicating the absence of hydrides.

Reaction with [$Ru_3(CO)_{12}$]

(*a*) When $(F_3CP)_4$ reacted with an equimolar amount of [$Ru_3(CO)_{12}$] at 120 °C in *p*-xylene a cubane 'cluster' **5** was obtained. The ^{19}F NMR spectrum showed signals at δ 20.67 (m) and a ^{31}P NMR signal was seen at δ −77.20 (m). Instead of the quartet signal expected for **5**, the ^{19}F NMR signal was distorted due to an effect known as 'virtual coupling'.[8] This

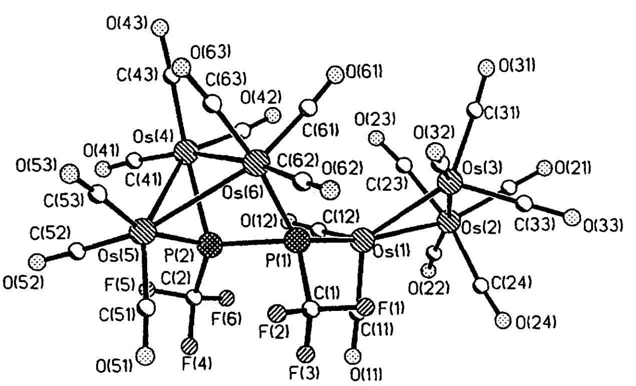

Fig. 1 Molecular structure of $[(OC)_9(\mu\text{-H})_2Os_3(\mu_4\text{-}F_3CPPCF_3)_9\text{-}Os_3(\mu\text{-H})_2(CO)_9]$ **3**

Table 1 Selected bond lengths (Å) and angles (°) for $[(OC)_9(\mu\text{-H})_2\text{-}Os_3(\mu_4\text{-}F_3CPPCF_3)Os_3(\mu\text{-H})_2(CO)_9]$ **3**

Os(1)–Os(2)	2.827(2)	Os(1)–Os(3)	2.692(2)
Os(2)–Os(3)	2.825(2)	Os(4)–Os(5)	2.943(2)
Os(4)–Os(6)	2.860(2)	Os(5)–Os(6)	3.024(2)
Os(1)–P(1)	2.379(7)	Os(4)–P(2)	2.347(8)
Os(5)–P(2)	2.349(8)	Os(6)–P(1)	2.485(7)
P(1)–P(2)	2.149(10)	P(1)–C(1)	1.909(36)
P(2)–C(2)	1.887(36)		
Os(3)–Os(1)–P(1)	103.0(2)	Os(1)–P(1)–P(2)	117.9(4)
Os(1)–P(1)–Os(6)	133.5(3)	Os(4)–P(2)–P(1)	102.2(4)
Os(5)–P(2)–P(1)	112.2(4)	Os(6)–P(1)–P(2)	80.4(3)

arose because the F atoms on the trifluoromethyl groups were coupled not only to the P atom to which the CF_3 was attached, but also with the adjacent P atom.

(*b*) When 2 equivalents of $[Ru_3(CO)_{12}]$ were used a pentaruthenium compound **6** arranged in a distorted octahedron with the phosphorus atom occupying the sixth octahedral site was obtained. The ^{19}F NMR spectrum showed a doublet at δ 21.72 [d, *J*(FP) = 73.4 Hz] while the ^{31}P NMR signal was at δ 408.27 [q, *J*(FP) = 73.5 Hz]. The large low-field shift of the ^{31}P NMR signal clearly points to a phosphorus environment of high co-ordination such as $\mu_4\text{-}PCF_3$.

(*c*) Using $(F_3CP)_4$ at 80 °C $[Ru_4(CO)_{14}(\mu_4\text{-}PCF_3)]$ **7** was obtained as a red band upon TLC of the reaction mixture. Red crystals were obtained from CH_2Cl_2–hexane solution at −20 °C. The ^{19}F NMR signal at δ 19.41 [d, *J*(FP) = 51.3 Hz] and the ^{31}P NMR signal at δ 73.07 [q, *J*(FP) = 52.5 Hz] indicated that only one type of F_3CP phosphinidene group is present in the molecule.

Reaction with $[Ru_4H_4(CO)_{12}]$

Reaction of $(F_3CP)_4$ with $[Ru_4H_4(CO)_{12}]$ at 70 °C in CH_2Cl_2 for 16 h gave $[Ru_4(\mu\text{-H})_2(CO)_{12}(\mu\text{-}PCF_3)(\mu_3\text{-}PCF_3)_2]$ **8** as orange crystals after purification by TLC and recrystallisation. The ^1H NMR spectrum gave two sets of signals at δ −14.50 [q, *J*(HP) = 7.1] and −14.70 [dt, *J*(HP) = 16.0, *J* = 5.2 Hz] with a relative intensity of 1 : 1. The ^{19}F NMR spectrum gave signals at δ 28.05 [d, *J*(FP) = 39.0] and 38.66 [d, *J*(FP) = 31.7 Hz] while the ^{31}P NMR spectrum gave signals at δ 75.08 [dq, *J*(PP) = 116.6, *J*(FP) = 34.0] and 223.35 [tq, *J*(PP) = 116.0, *J*(FP) = 29.2 Hz]. The ^{31}P signal at δ 223.35 is unusual because it would be too low field for a $\mu_3\text{-}PCF_3$[9] but not low field enough to be a $\mu_4\text{-}PCF_3$ as observed in compound **6**. This low-field shift is caused by a rare trigonal-pyramidal $\mu\text{-}PCF_3$ structure.

Reactions using $(F_3CP)_5$

The pentameric cyclophosphane $(F_3CP)_5$ was used in place of the tetramer in reactions with (*a*) $[Os_3(CO)_{11}(MeCN)]$ at 80 °C, (*b*) $[Os_3(\mu\text{-H})_2(CO)_{10}]$ at 80 °C, (*c*) $[Ru_3(CO)_{12}]$ at 80 °C and (*d*) $[Ru_4H_4(CO)_{12}]$ at 70 °C. The products isolated were identical to those obtained when the tetramer was used. All cluster derivatives identified showed cleavage of the cyclophosphane ring. This is in contrast to our earlier work.[5,6]

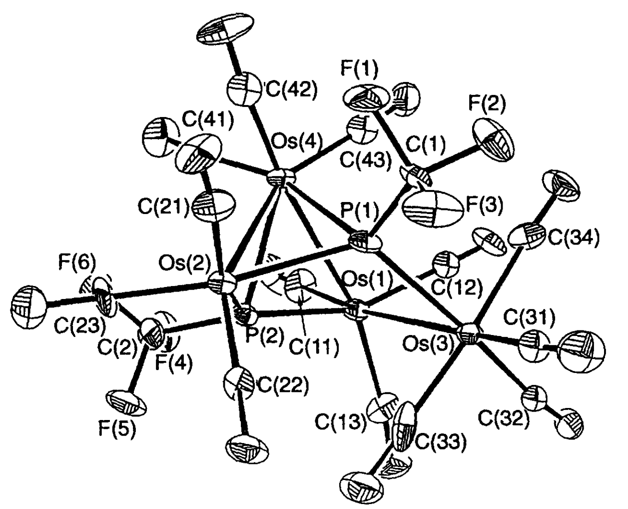

Fig. 2 Molecular structure of $[Os_4(CO)_{13}(\mu_3\text{-}PCF_3)_2]$ **4**

Table 2 Selected bond lengths (Å) and angles (°) for $[Os_4(CO)_{13}\text{-}(\mu_3\text{-}PCF_3)_2]$ **4**

Os(1)–Os(3)	2.944(4)	Os(1)–Os(4)	2.985(4)
Os(1)–P(2)	2.342(8)	Os(2)–P(1)	2.401(8)
Os(2)–P(2)	2.336(8)	Os(3)–P(1)	2.437(9)
Os(4)–P(1)	2.414(8)	Os(4)–P(2)	2.420(8)
Os(3)–Os(1)–Os(4)	88.2(1)	Os(1)–Os(4)–Os(2)	91.9(1)
Os(2)–P(1)–Os(4)	74.6(2)	Os(2)–P(1)–Os(3)	123.9(3)
Os(3)–P(1)–Os(4)	116.5(3)	Os(1)–P(2)–Os(2)	130.1(3)
Os(1)–P(2)–Os(4)	77.6(2)	Os(2)–P(2)–Os(4)	75.6(2)

Infrared spectra of compounds 1–8

The carbonyl stretching vibrations of all of the compounds obtained generally fall in the region between 1900 and 2200 cm^{-1}. These represent an increase of about 100 cm^{-1} compared with those of other osmium and ruthenium compounds containing non-fluorinated phosphane ligands.[10] This is due to the greater π-acidity of the trifluoromethyl ligands as a result of the electron-withdrawing effect of the CF_3 groups. The IR spectra also showed C–F stretching vibration at around 1100–1200 cm^{-1}, typical of trifluoromethylated phosphane compounds. However, the C–F deformation modes were not observed due to low intensity.

Molecular structures

$[(OC)_9(\mu\text{-H})_2Os_3(\mu_4\text{-}F_3CPPCF_3)Os_3(\mu\text{-H})_2(CO)_9]$ 3. Compound **3** (Fig. 1, Table 1) consists of a butterfly framework made up by Os(4), Os(5), Os(6) and P(2). The wing-tips Os(6) and P(2) are bridged by P(1), which is also linked to the osmium triangle Os(1), Os(2) and Os(3) through Os(1). Though the hydrides in **3** were not located in the X-ray crystallographic study, their presence is confirmed by ^1H NMR spectroscopy and their location assigned based on the metal–metal bond lengths. It has been shown that the presence of a μ-H bridge on a triosmium cluster results in lengthening of an Os–Os bond.[11] One hydride most probably bridges the Os(4)–Os(5) edge while the other is located across the Os(5)–Os(6) bond [2.943(2) and 3.024(2) Å respectively]. The Os(1)–Os(3) bond is exceptionally short and can be assigned as an Os=Os bond with two bridging

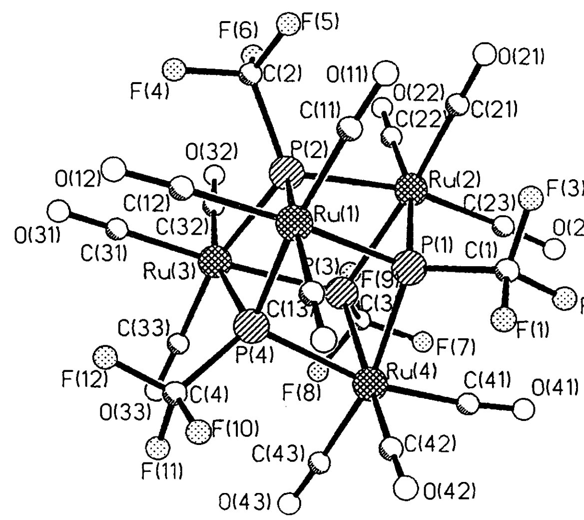

Fig. 3 Molecular structure of [{Ru(CO)$_3$(μ_3-PCF$_3$)}$_4$] **5**

Table 3 Selected bond lengths (Å) and angles (°) for [{Ru(CO)$_3$-(μ_3-PCF$_3$)}$_4$] **5**

Ru(1)–P(1)	2.398(3)	Ru(1)–P(2)	2.407(2)
Ru(1)–P(4)	2.402(2)	Ru(2)–P(1)	2.390(3)
Ru(2)–P(2)	2.414(3)	Ru(2)–P(3)	2.413(2)
Ru(3)–P(2)	2.404(2)	Ru(3)–P(3)	2.409(2)
Ru(3)–P(4)	2.421(2)	Ru(4)–P(1)	2.384(2)
Ru(4)–P(3)	2.405(2)	Ru(4)–P(4)	2.404(3)
P(1)–C(1)	1.865(10)	P(2)–C(2)	1.898(10)
P(3)–C(3)	1.878(10)	P(4)–C(4)	1.868(11)
P(1)–Ru(1)–P(2)	74.3(1)	P(1)–Ru(1)–P(4)	74.2(1)
P(2)–Ru(1)–P(4)	74.5(1)	P(1)–Ru(2)–P(2)	74.3(1)
P(1)–Ru(2)–P(3)	74.4(1)	P(2)–Ru(2)–P(3)	73.7(1)
P(2)–Ru(2)–P(3)	74.0(1)	P(2)–Ru(3)–P(4)	74.2(1)
P(3)–Ru(3)–P(4)	74.3(1)	P(1)–Ru(4)–P(3)	74.6(1)
P(1)–Ru(4)–P(4)	74.4(1)	P(3)–Ru(4)–P(4)	74.7(1)
Ru(1)–P(1)–Ru(2)	104.1(1)	Ru(1)–P(1)–Ru(4)	104.2(1)
Ru(2)–P(1)–Ru(4)	104.0(1)	Ru(1)–P(2)–Ru(2)	103.1(1)
Ru(1)–P(2)–Ru(3)	103.8(1)	Ru(2)–P(2)–Ru(3)	104.4(1)
Ru(2)–P(3)–Ru(3)	104.3(1)	Ru(2)–P(3)–Ru(4)	102.7(1)
Ru(3)–P(3)–Ru(4)	103.8(1)	Ru(1)–P(4)–Ru(3)	103.4(1)
Ru(1)–P(4)–Ru(4)	103.4(1)	Ru(3)–P(4)–Ru(4)	103.4(1)

hydrides. Thus we have a cluster with the diphosphinidene ligand bridging 48- and a 46-electron triosmium moieties. The P(1)–P(2) bond length is 2.149(10) Å, significantly shorter than that of the parent *cyclo*-(F$_3$CP)$_4$ [2.213(5) Å].[12] In fact, the bond length is more similar to the P=P double bonds reported in compounds such as [Pd(η^2-CF$_3$P=PCF$_3$)(PPh$_3$)$_2$] [2.121(2) Å],[13] [Pd(η^2-PhP=PPh)(dppe)] [2.121(4) Å][14] and shorter than in [Pt(η^2-C$_6$F$_5$P=PC$_6$F$_5$)(PPh$_3$)$_2$] [2.156(7) Å].[15] As such, the bond between P(1) and P(2) can be considered to be an exceptionally short single bond, probably with partial double-bond character.

[Os$_4$(CO)$_{13}$(μ_3-PCF$_3$)$_2$] 4. Compound **4** (Fig. 2, Table 2) consists of an open chain of four osmium atoms with two μ_3-PCF$_3$ groups each bridging three Os atoms. Each Os atom has three axial CO groups except one of the chain-end Os atoms which has four. The Os–Os bond length varies narrowly between 2.917 and 2.985 Å. All the Os–Os bond lengths of this open-chain cluster are longer than the average Os–Os distance of 2.877 Å for the parent [Os$_3$(CO)$_{12}$].[11] The Os–P bond lengths, however, show larger differences with the shortest being Os(2)–P(2) [2.336(8) Å] and the longest [Os(3)–P(1) 2.437(9) Å]. All CO groups are terminally bonded to the Os atoms with all Os–C–O bond angles being almost linear, giving an average of 173°.

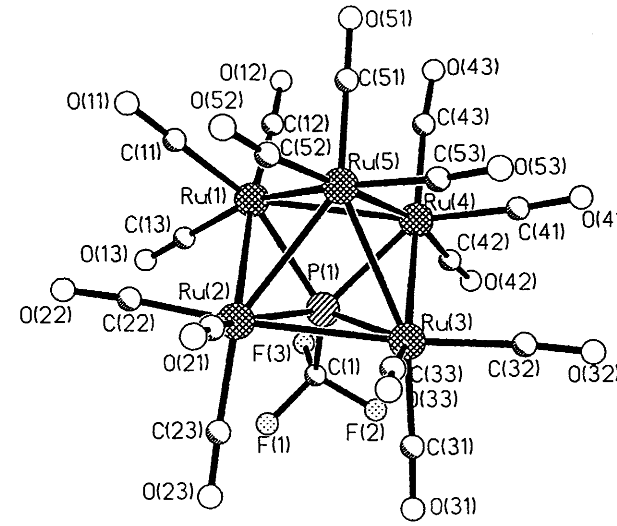

Fig. 4 Molecular structure of [Ru$_5$(CO)$_{15}$(μ_4-PCF$_3$)] **6**

Table 4 Selected bond lengths (Å) and angles (°) for [Ru$_5$(CO)$_{15}$-(μ_4-PCF$_3$)] **6**

Ru(1)–Ru(2)	2.896(1)	Ru(1)–Ru(4)	2.954(1)
Ru(1)–Ru(5)	2.808(1)	Ru(2)–Ru(3)	2.877(1)
Ru(2)–Ru(5)	2.890(1)	Ru(3)–Ru(5)	2.855(1)
Ru(4)–Ru(5)	2.820(1)	Ru(1)–P(1)	2.347(2)
Ru(2)–P(1)	2.330(2)	Ru(3)–P(1)	2.343(2)
Ru(4)–P(1)	2.333(2)	P(1)–C(1)	1.887(6)
Ru(2)–Ru(1)–Ru(4)	89.6(1)	Ru(2)–Ru(1)–Ru(5)	60.9(1)
Ru(4)–Ru(1)–Ru(5)	58.5(1)	Ru(1)–Ru(2)–Ru(3)	91.1(1)
Ru(1)–Ru(2)–Ru(5)	58.1(1)	Ru(3)–Ru(2)–Ru(5)	59.4(1)
Ru(2)–Ru(3)–Ru(4)	90.4(1)	Ru(2)–Ru(3)–Ru(5)	60.5(1)
Ru(4)–Ru(3)–Ru(5)	58.3(1)	Ru(1)–Ru(4)–Ru(5)	58.1(1)
Ru(3)–Ru(4)–Ru(5)	59.5(1)	Ru(1)–Ru(4)–Ru(3)	88.8(1)
Ru(1)–Ru(5)–Ru(2)	61.1(1)	Ru(1)–Ru(5)–Ru(3)	93.3(1)
Ru(2)–Ru(5)–Ru(3)	60.1(1)	Ru(1)–Ru(5)–Ru(4)	63.3(1)
Ru(2)–Ru(5)–Ru(4)	92.5(1)	Ru(3)–Ru(5)–Ru(4)	62.2(1)
Ru(1)–P(1)–Ru(2)	76.5(1)	Ru(1)–P(1)–Ru(3)	122.9(1)
Ru(2)–P(1)–Ru(3)	76.0(1)	Ru(1)–P(1)–Ru(4)	78.3(1)
Ru(2)–P(1)–Ru(4)	124.4(1)	Ru(3)–P(1)–Ru(4)	77.7(1)
Ru(1)–P(1)–C(1)	118.1(2)	Ru(2)–P(1)–C(1)	119.4(2)
Ru(3)–P(1)–C(1)	119.0(2)	Ru(4)–P(1)–C(1)	116.2(2)

Table 5 Selected bond lengths (Å) and angles (°) for [Ru$_4$(CO)$_{14}$-(μ_4-PCF$_3$)] **7**

Ru(1)–Ru(3)	2.959(1)	Ru(2)–Ru(3)	2.910(1)
Ru(2)–Ru(4)	2.801(1)	Ru(3)–Ru(4)	2.893(1)
Ru(5)–Ru(7)	2.971(1)	Ru(6)–Ru(7)	2.874(1)
Ru(6)–Ru(8)	2.817(1)	Ru(7)–Ru(8)	2.886(1)
Ru(1)–P(1)	2.373(1)	Ru(2)–P(1)	2.327(1)
Ru(3)–P(1)	2.877(1)	Ru(4)–P(1)	2.339(1)
Ru(5)–P(2)	2.375(1)	Ru(6)–P(2)	2.331(1)
Ru(7)–P(2)	2.864(2)	Ru(8)–P(2)	2.323(2)
Ru(3)–C(34)–O(34)	161.2(5)	Ru(3)–C(33)–Ru(4)	79.9(2)
Ru(6)–C(74)–Ru(7)	79.4(2)	Ru(7)–C(73)–Ru(8)	77.5(2)

[{Ru(CO)$_3$(μ_3-PCF$_3$)}$_4$] 5. Compound **5** (Fig. 3, Table 3) is a 80-electron 'cluster' arranged in a distorted cuboid structure with the skeleton made up of alternating P and Ru atoms. It is a highly symmetrical molecule with three terminally bonded carbonyls on each Ru atom. The average P–Ru–P angle is 74.4° while that of Ru–P–Ru is 103.9° which agrees well with the structure of [{Fe(CO)$_3$(AsMe)}$_4$],[16] the only other X-ray characterised Group 8–Group 5 cubane. The smaller angle at Ru compared to P is probably due to crowding since the Ru is also bonded to three other CO groups while the P atom only has one CF$_3$ group attached.

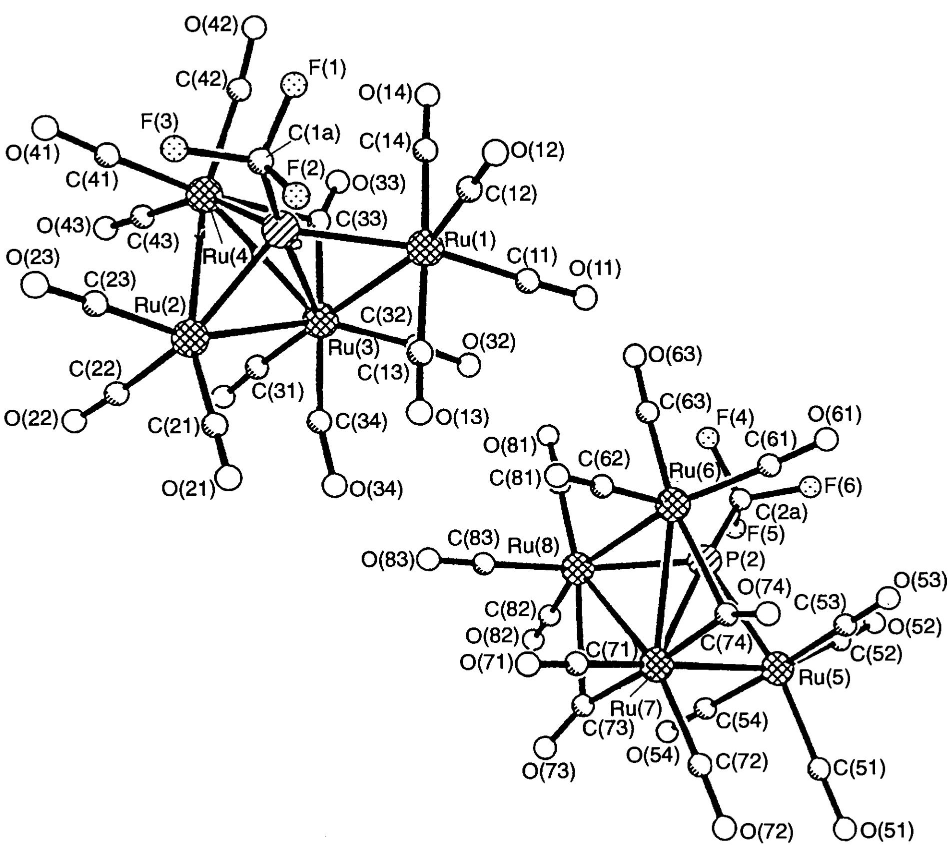

Fig. 5 Molecular structure of $[Ru_4(CO)_{14}(\mu_4\text{-}PCF_3)]$ **7**

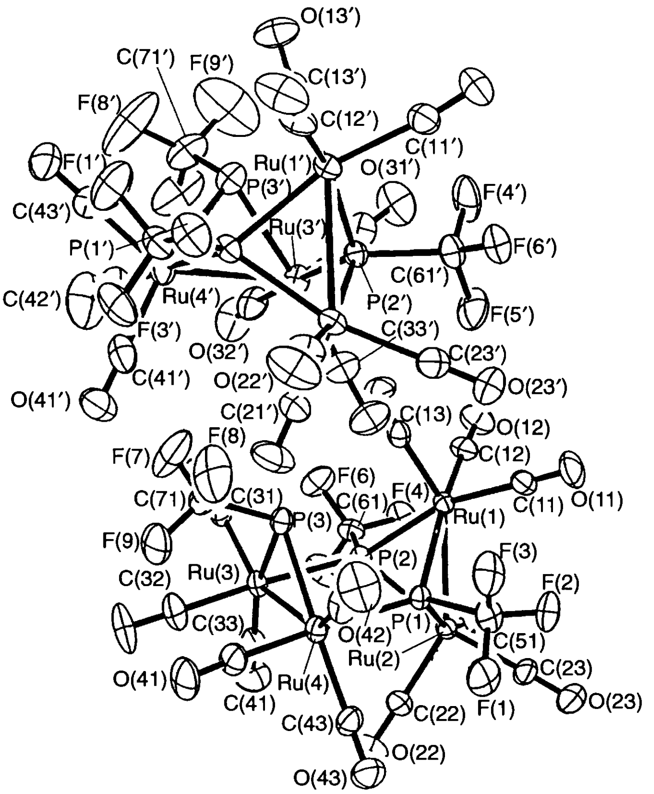

Fig. 6 Molecular structure of $[Ru_4(\mu\text{-}H)_2(CO)_{12}(\mu\text{-}PCF_3)(\mu_3\text{-}PCF_3)_2]$ **8**

$\mathbf{[Ru_5(CO)_{15}(\mu_4\text{-}PCF_3)]}$ **6.** Complex **6** (Fig. 4, Table 4), has the same structure as that of the series of four mono(organo) phosphido-bridged pentaruthenium carbonyl clusters $[Ru_5(CO)_{15}(\mu\text{-}PR)]$ prepared by Huttner and co-workers[17] using $[Ru_3(CO)_{12}]$ and $[Mn(C_5H_5)(CO)_2(PRCl_2)]$ (R = Ph, Et, Me or CH_2Ph). This compound has an octahedral core made up of five Ru and a P atom occupying one of the apices. Each Ru atom has three terminal CO groups bonded to it. The average Ru–P bond length is 2.34 Å and that of Ru–Ru is 2.88 Å.

$\mathbf{[Ru_4(CO)_{14}(\mu_4\text{-}PCF_3)]}$ **7.** Complex **7** (Fig. 5, Table 5) is a tetraruthenium cluster with a M_4 metal framework having the trifluoromethylphosphinidene interacting with all four ruthenium atoms. It has two independent molecules per unit cell, one with a bridging carbonyl and a bent semibridging carbonyl,[18] the other with two bridging carbonyls. Complex **7** also exhibits some of the longest Ru–P bonds in Ru(3)–P(1) and Ru(7)–P(2) of 2.877(1) and 2.864(2) Å respectively. Crabtree and Lavin,[19] in a statistical analysis of 35 iron carbonyl compounds containing semibridging CO ligands, derived the empirical relationship $\theta = n\psi + m$. They obtained the values $n = 1.51$ and $m = 64.5$. In our study, $n = 1.53$ and $m = 64.7$.

$\mathbf{[Ru_4(\mu\text{-}H)_2(CO)_{12}(\mu\text{-}PCF_3)(\mu_3\text{-}PCF_3)_2]}$ **8.** Complex **8** (Fig. 6, Table 6) consists of a butterfly structure made up of Ru(1) and Ru(2) as the hinges and P(1) and P(2) as the wing-tips. This structure is further linked to a triangle consisting of Ru(3)–Ru(4)–P(3) through the wing-tips P(1) and P(2) to Ru(4) and Ru(3) respectively. Each Ru atom has three terminally bonded CO groups. Both P(1) and P(2) have μ_3 bonding modes, while P(3) is a rare μ-bonded phosphorus. Atom P(3) shows a trigonal-pyramidal geometry with the lone pair of electrons most likely extending perpendicular to the plane comprising Ru(3), Ru(4) and the CF_3 group. This lone pair of electrons exert a force on the nearest CO group, *i.e.* C(13)–O(13), and as a result the C(13)–O(13) is bent out of linearity [169.7(10)°]. It is possible that this close proximity of the CO to the lone pair on the P atom is able to provide enough shielding to prevent this very active lone pair from further reactions with other species.

Table 6 Selected bond lengths (Å) and angles (°) for $[Ru_4(\mu\text{-}H)_2(CO)_{12}(\mu\text{-}PCF_3)(\mu_3\text{-}PCF_3)_2]$ **8**

Ru(1)–Ru(2)	2.857(2)	Ru(3)–Ru(4)	2.967(2)
Ru(1')–Ru(2')	2.863(2)	Ru(3')–Ru(4')	2.980(2)
Ru(1)–P(1)	2.400(3)	Ru(2)–P(1)	2.389(3)
Ru(1')–P(1')	2.388(3)	Ru(2')–P(1')	2.394(3)
Ru(4)–P(1)	2.437(3)	Ru(1)–P(2)	2.390(3)
Ru(4')–P(1')	2.449(3)	Ru(1')–P(2')	2.398(3)
Ru(2)–P(2)	2.398(3)	Ru(3)–P(2)	2.450(3)
Ru(2')–P(2')	2.390(3)	Ru(3')–P(2')	2.422(3)
Ru(3)–P(3)	2.417(3)	Ru(4)–P(3)	2.403(3)
Ru(3')–P(3')	2.409(3)	Ru(4')–P(3')	2.424(3)
Ru(1)–C(13)–O(13)	169.1(10)	Ru(3)–P(3)–Ru(4)	76.0(1)
Ru(1')–C(13')–O(13')	169.4(10)	Ru(3')–P(3')–Ru(4')	76.1(1)
Ru(3)–P(3)–C(71)	109.3(4)	Ru(4)–P(3)–C(71)	110.6(4)
Ru(3')–P(3')–C(71')	110.3(5)	Ru(4')–P(3')–C(71')	108.7(5)

Conclusion

In contrast to our earlier work with $(PhP)_5$,[5,6] the reactions of *cyclo*-$(F_3CP)_4$ and *cyclo*-$(F_3CP)_5$ with osmium carbonyl clusters proceeded *via* cleavage of the phosphorus rings. The reactive F_3CP and $(F_3CP)_2$ species generated were captured by the triosmium carbonyl clusters resulting in the formation of compounds **1–3**. However, in the reactions with ruthenium carbonyl clusters at elevated temperatures, both the clusters $[Ru_3(CO)_{12}]$ and $[Ru_4H_4(CO)_{12}]$ and the cyclophosphanes underwent ring rupture to afford new ruthenium carbonyl cluster derivatives **5–8**.

Experimental

As $(F_3CP)_n$ (n = 4 or 5) are pyrophoric in air, the syntheses and handling were carried out using an all-glass vacuum line equipped with Teflon gas-tight taps. All the reactions were performed *in vacuo* in a double reaction vessel equipped with Teflon taps. Cluster derivatives were recrystallised under an atmosphere of dry, oxygen-free nitrogen. The solvents used, namely, CH_2Cl_2, hexane and xylene, were distilled prior to use under a nitrogen atmosphere over the appropriate drying agent.[20] Products were separated by TLC using laboratory-prepared 20 × 20 cm glass plates coated to 0.3 mm thickness with Merck-Kieselgel $60F_{254}$ silica gel. The IR spectra were recorded on a Perkin-Elmer 983G spectrometer, NMR spectra on either a Bruker ACF-300 or JEOL FX -90Q FT spectrometer; $SiMe_4$ trifluoroacetic acid and H_3PO_4 were employed as external references for ^1H, ^{19}F and ^{31}P NMR respectively and $CDCl_3$ was used as the solvent. The following compounds were prepared by literature methods: $[Os_3(CO)_{12}]$,[21] $[Os_3(CO)_{11}(MeCN)]$,[22] $[Os_3(\mu\text{-}H)_2(CO)_{10}]$,[23] $[Ru_3(CO)_{12}]$,[24] $[Ru_4(\mu\text{-}H)_4(CO)_{12}]$[25] and $(F_3CP)_n$[26] (n = 4 or 5).

Reactions of $(F_3CP)_n$ (n = 4 or 5) with clusters

(*a*) With $[Os_3(CO)_{11}(MeCN)]$. The compound $(F_3CP)_4$ (0.1320 g, 0.330 mmol) was condensed into a degassed solution of $[Os_3(CO)_{11}(MeCN)]$ (0.2590 g, 0.282 mmol) at liquid-nitrogen temperature. The reaction mixture was allowed to warm to room temperature and then heated with stirring in CH_2Cl_2 at 80 °C for 16 h. The resulting dark yellow solution was evaporated to dryness. The residue was dissolved in the minimum volume of CH_2Cl_2 and separated by TLC at room temperature using hexane–CH_2Cl_2 (70:30) to give a yellow band (R_f = 0.65) of complex **1** (*ca.* 35 mg, 12%) (Found: C, 14.8; H, 0.15; P, 1.55. Calc. for $C_{23}H_2F_3O_{22}Os_6P$: C, 14.85; H, 0.10; P, 1.65%). Orange crystals were obtained by recrystallisation from dichloromethane–hexane solution at −20 °C. ^1H NMR: δ 5.95 [dq, J(HP) = 334.6, J(HF) = 9.4] and −19.32 [d, J(HP) = 9.4 Hz]. IR: $\tilde{\nu}$(CO)/cm^{-1} 2146w, 2109m, 2100s, 2076 (sh), 2064vs, 2055 (sh), 2022vs and 1934w. When $(F_3CP)_4$ was replaced with $(F_3CP)_5$ the reaction proceeded in the same manner.

(*b*) With $[Os_3(\mu\text{-}H)_2(CO)_{10}]$. The compound $(F_3CP)_4$ (0.1350 g, 0.338 mmol) was condensed into a degassed solution of $[Os_3(\mu\text{-}H)_2(CO)_{10}]$ (0.2700 g, 0.316 mmol) in hexane. The mixture was heated to 80 °C and stirred for 16 h. The reaction proceeded slowly, with the initial purple solution turning yellow and then brown. The solution was evaporated to dryness and separated by TLC using hexane–CH_2Cl_2 (70:30) as eluent to give a yellow band (R_f = 0.83) of complex **2** (*ca.* 10 mg, 4%) (Found: C, 13.95; H, 0.05; P, 3.25. Calc. for $C_{11}H_2F_3O_{10}Os_3P$: C, 13.85; H, 0.20; P, 3.25%) and a red band (R_f = 0.34) of **3** (*ca.* 8 mg, 2%) (Found: C, 12.65; H, 0.00; P, 3.35. Calc. for $C_{20}H_4F_6O_{18}Os_6P_2$: C, 13.0; H, 0.20; P, 3.35%). Crystals of **2** and **3** suitable for X-ray analysis were obtained by recrystallisation from the CH_2Cl_2–hexane solutions at −20 °C. Complex **2**: ^1H NMR δ 6.76 [ddq, J(HP) = 433.6, J(FH) = 7.7, J(HH) = 4.3] and −20.38 [dd, J(HP) = 17.8, J(HH) = 4.3]; ^{19}F NMR δ 18.86 [dd, J(FP) = 68.4, J(FH) = 7.3]; ^{31}P NMR δ 25.03 [q, J(PF) = 68.4 Hz]; IR $\tilde{\nu}$(CO)/cm^{-1} 2112w, 2074vs, 2064s, 2031s, 2014vs and 1992w. Complex **3**: IR $\tilde{\nu}$(CO)/cm^{-1} 2129w, 2101m, 2094w, 2077s, 2059s, 2034m, 2017s, 1996vw, 1985w and 1978vw. The reaction was repeated using $(F_3CP)_5$ and the same products were isolated.

(*c*) With $[Os_3(CO)_{12}]$. The compound $[Os_3(CO)_{12}]$ (0.3203 g, 0.353 mmol) and $(F_3CP)_4$ (0.1602 g, 0.400 mmol) were heated in a sealed tube at 209 °C for 16 h. After removing the volatiles under vacuum, the black residue was taken up in the minimum volume of CH_2Cl_2 and separated by TLC using hexane–CH_2Cl_2 (90:10) as eluent to give a yellow band (R_f = 0.34) of complex **4** (*ca.* 25 mg, 10%) (Found: C, 13.6; P, 4.75. Calc. for $C_{15}F_6O_{13}Os_4P_2$: C, 13.6; P, 4.70%). Cooling a CH_2Cl_2–hexane solution of **4** at −20 °C yielded yellow crystals suitable for X-ray analysis. IR: $\tilde{\nu}$(CO)/cm^{-1} 2128w, 2095s, 2073vs, 2059s, 2055s, 2048m, 2036m, 2012m and 2002w.

(*d*) With $[Ru_3(CO)_{12}]$ (1:1 molar ratio). The compound $[Ru_3(CO)_{12}]$ (0.2440 g, 0.382 mmol) and $(F_3CP)_4$ (0.1394 g, 0.347 mmol) were heated with continuous stirring in xylene at 120 °C for 4 h. The reaction mixture turned brown from the initial light orange. Dissolution of all the $[Ru_3(CO)_{12}]$ used indicated that the reaction was complete. The solution was evaporated to dryness under vacuum and separated by TLC using hexane–CH_2Cl_2 (90:10) to give a yellow band (R_f = 0.83) of complex **5** (*ca.* 12 mg, 4%) (Found: C, 17.0; P, 10.75. Calc. for $C_{16}F_{12}O_{12}P_4Ru_4$: C, 16.85; P, 10.85%.) Cooling a CH_2Cl_2–hexane solution of **5** at −20 °C afforded yellow crystals suitable for X-ray analysis. IR: $\tilde{\nu}$(CO)/cm^{-1} 2096s, 2077w, 2051w and 2031w.

(*e*) With $[Ru_3(CO)_{12}]$ (1:2 molar ratio). The compound $[Ru_3(CO)_{12}]$ (0.2571 g, 0.402 mmol) and $(F_3CP)_4$ (0.0822 g, 0.205 mmol) were heated with stirring in xylene at 120 °C for 7 h. The solution was evaporated to dryness under vacuum and separated by TLC at room temperature using hexane–CH_2Cl_2 (95:5) as eluent to give a green band (R_f = 0.56) of complex **6** (*ca.* 20 mg, 5%) (Found: C, 18.6; P, 2.80. Calc. for $C_{16}F_3O_{15}PRu_5$: C, 18.75; P, 3.00%). Green crystals of **6** suitable for X-ray analysis were obtained from a CH_2Cl_2–hexane solution at −20 °C. IR: $\tilde{\nu}$(CO)/cm^{-1} 2122w, 2087m, 2060s and 2024w.

(*f*) With $[Ru_3(CO)_{12}]$ at 80 °C (1:1 molar ratio). The compound $(F_3CP)_4$ (0.1330 g, 0.333 mmol) was condensed at liquid-nitrogen temperature into a CH_2Cl_2 solution of $[Ru_3(CO)_{12}]$ (0.1800 g, 0.281 mmol). The mixture was heated

Table 7 Crystallographic data for complexes **3–8**

	3	**4**	**5**	**6**	**7**	**8**
Formula	$C_{20}H_4F_6O_{18}Os_6P_2$	$C_{15}F_6O_{13}Os_4P_2$	$C_{16}F_{12}O_{12}P_4Ru_4$	$C_{16}F_3O_{15}PRu_5$	$C_{15}F_3O_{14}PRu_4$	$C_{15}H_2F_9O_{12}P_3Ru_4$
M	1845.4	1324.9	1140.3	2051.0	896.4	1040.3
Crystal size/mm	0.25 × 0.30 × 0.35	0.40 × 0.30 × 0.30	0.30 × 0.30 × 0.20	0.30 × 0.20 × 0.10	0.40 × 0.20 × 0.20	0.50 × 0.30 × 0.10
Crystal system	Monoclinic	Monoclinic	Monoclinic	Monoclinic	Triclinic	Monoclinic
Space group	$P2_1/c$	$C2/c$	$P2_1/c$	$P2_1/n$	$P\bar{1}$	$P2_1/n$
a/Å	10.568(4)	18.26(3)	10.400(5)	10.104(4)	9.9380(10)	14.662(6)
b/Å	16.316(3)	9.776(5)	10.522(5)	21.267(6)	16.475(2)	22.427(10)
c/Å	20.489(10)	29.79(3)	28.744(6)	11.854(5)	16.764(3)	17.710(8)
α/°					108.890(10)	
β/°	95.31(3)	96.87(10)	90.000(0)	92.74(3)	100.649(10)	95.080(0)
γ/°					102.650(10)	
U/Å^3	3518(2)	5280(9)	3145.4(14)	2544.3(16)	2434.8(6)	5801(4)
Z	8	8	4	2	4	8
D_c/g cm^{-3}	3.484	3.333	2.408	2.677	2.445	2.382
μ(Mo-Kα)/cm^{-1}	217.8	194.1	221.1	305.6	258.8	231.9
ω scan width/°	1.20	1.20	1.20	1.20	1.20	1.00
Measured reflections	6688	4624	3136	4858	9037	10 586
Independent reflections	6099	4489	2965	4451	8506	10 238
Observed reflections [$F_o > 4\sigma(F_o)$]	3922	3344	2488	3831	7039	6521
Absorption correction (minimum, maximum)	0.1511, 1.0000	0.0995, 0.2023	0.1419, 0.1684	0.1320, 0.1778	0.3637, 0.4349	0.1027, 0.1439
R	0.0665	0.073	0.0287	0.0280	0.0267	0.0471
R'*	0.0804	0.0947	0.0315	0.0358	0.0274	0.0833
Goodness of fit	1.42	1.85	1.67	1.50	1.25	1.04

* Weighting scheme $w^{-1} = \sigma^2(F) + 0.0010F^2$.

at 80 °C for 16 h with the orange solution gradually turning red. Upon cooling to room temperature the solution was evaporated to dryness and separated by TLC using hexane–CH_2Cl_2 (90:10) to give a red band of complex **7** (*ca.* 10 mg, 4%). Red crystals of **7** suitable for X-ray analysis were obtained from a CH_2Cl_2–hexane solution at −20 °C. IR: $\tilde{\nu}$(CO)/cm^{-1} 2095vw, 2067s, 2041m and 2004vw. The experiment was repeated using $(F_3CP)_5$ in exactly the same manner yielding the same results.

***(g)* With $[Ru_4(\mu\text{-}H)(CO)_{12}]$.** The reaction using tetra- or penta-meric cyclophosphane proceeded in the same way. Only that using $(F_3CP)_4$ is described. The compounds $[Ru_4(\mu\text{-}H)_4(CO)_{12}]$ (0.2527 g, 0.339 mmol) and $(F_3CP)_4$ (0.1560 g, 0.390 mmol) were heated in CH_2Cl_2 at 70 °C. The solution turned brown after 2 h but was heated for a total of 16 h. The mixture was evaporated to dryness under vacuum and separated by TLC using hexane–CH_2Cl_2 (85:15) to give a yellow band (R_f = 0.50) of complex **8** (*ca.* 21 mg, 8%) (Found: C, 17.3; H, 0.15; P, 8.85. Calc. for $C_{15}H_2F_9O_{12}P_3Ru_4$: C, 17.25; H, 0.20; P, 8.90%). Orange crystals of **8** suitable for X-ray analysis were obtained from a CH_2Cl_2–hexane solution at −20 °C. IR: $\tilde{\nu}$(CO)/cm^{-1} 2110vw, 2103s, 2097vs, 2091m, 2081m, 2067vs, 2059s, 2052m, 2044w, 2031m and 2025m.

Crystallography

Crystal data and details of measurements for complexes **3**–**8** are in Table 7. Diffraction intensities were collected at 298 K on a Siemens R3m/V diffractometer, using the ω-scan mode with graphite-monochromated Mo-Kα radiation (λ = 0.071 73 Å). All computations were carried out using the SHELXTL PLUS[27] PC VERSION program package. The structures were solved by direct methods for the osmium and ruthenium atoms and Fourier-difference techniques for the remaining non-hydrogen atoms. Refinement was by the full-matrix least-squares method on F^2 with all non-hydrogen atoms anisotropic.

Atomic coordinates, thermal parameters, and bond lengths and angles have been deposited at the Cambridge Crystallographic Data Centre (CCDC). See Instructions for Authors, *J. Chem. Soc., Dalton Trans.*, 1996, Issue 1. Any request to the CCDC for this material should quote the full literature citation and the reference number 186/101.

References

1 H. G. Ang, J. S. Shannon and B. O. West, *Chem. Commun.*, 1965, 10.
2 H. G. Ang and B. O. West, *Aust. J. Chem.*, 1967, **20**, 1133.
3 B. F. G. Johnson, T. M. Layer, J. Lewis, P. R. Raithby and W. T. Wong, *J. Chem. Soc., Dalton Trans.*, 1993, 973.
4 E. Charalambous, L. Heuer, B. F. G. Johnson, J. Lewis, W. S. Li, M. McPartlin and A. D. Massey, *J. Organomet. Chem.*, 1994, **468**, C9.
5 H. G. Ang, S. G. Ang, W. L. Kwik and Q. Zhang, *J. Organomet. Chem.*, 1995, **485**, C10.
6 H. G. Ang, L. L. Koh and Q. Zhang, *J. Chem. Soc., Dalton Trans.*, 1995, 2757.
7 H. G. Ang, C. H. Koh, L. L. Koh, W. L. Kwik, W. K. Leong and W. Y. Leong, *J. Chem. Soc., Dalton Trans.*, 1993, 847.
8 R. H. Crabtree, *The Organometallic Chemistry of the Transition Metals*, Wiley, New York, 1988, ch. 10, p. 214.
9 G. Hutter and K. Knoll, *Angew. Chem., Int. Ed. Engl.*, 1987, **26**, 743.
10 M. I. Bruce and M. J. Liddel, *J. Organomet. Chem.*, 1988, **347**, 157.
11 M. R. Churchill and B. G. Deboer, *Inorg. Chem.*, 1977, **16**, 878.
12 G. J. Palenik and J. Donahue, *Acta Crystallogr.*, 1962, **15**, 564.
13 I. G. Phillips, R. G. Ball and R. G. Cavell, *Inorg. Chem.*, 1992, **31**, 1633.
14 J. Chatt, P. B. Hitchcock, A. Pidcock, C. P. Warrens and K. R. Dixon, *J. Chem. Soc., Chem. Commun.*, 1982, 932; *J. Chem. Soc., Dalton Trans.*, 1984, 2237.
15 P. S. Elmes, M. L. Scudder and B. O. West, *J. Organomet. Chem.*, 1976, **122**, 281.
16 E. Rottinger and H. Vahrenkamp, *Angew. Chem., Int. Ed. Engl.*, 1978, **17**, 273.
17 K. Natarajan, L. Zsolnai and G. Huttner, *J. Organomet. Chem.*, 1981, **209**, 85.
18 A. L. Rheingold, B. S. Haggerty, G. L. Geoffroy and S. H. Han, *J. Organomet. Chem.*, 1990, **384**, 209.
19 R. H. Crabtree and M. Lavin, *Inorg. Chem.*, 1986, **25**, 805.
20 A. I. Vogel, *Vogel's Textbook of Practical Organic Chemistry*, 5th edn., Longman, London, 1989, ch. 4, pp. 396–411.
21 B. F. G. Johnson and J. Lewis, *Inorg. Synth.*, 1972, **13**, 93.
22 J. N. Nicholls and M. D. Varges, *Inorg. Synth.*, 1989, **26**, 290.
23 E. Sappa and M. Valle, *Inorg. Synth.*, 1989, **26**, 367.
24 M. I. Bruce, C. M. Jensen and N. L. Jones, *Inorg. Synth.*, 1989, **26**, 259.
25 M. I. Bruce and M. L. Williams, *Inorg. Synth.*, 1989, **26**, 262.
26 W. Mahler and A. B. Burg, *J. Am. Chem. Soc.*, 1958, **80**, 6161.
27 G. M. Sheldrick, Siemens Analytical Instruments, Madison, WI, 1986.

Received 18*th December* 1995; *Paper* 5/08202A